Four-Wave Mixing Between Pump and Signal in a Distributed Raman Amplifier

Tsu-Te Kung, Ching-Ten Chang, *Member, IEEE,* Jeng-Cherng Dung, and Sien Chi, *Fellow, OSA*

***Abstract*—We observed experimentally four-wave mixing (FWM) between a 14xx-nm pump and a 15xx-nm signal in a forward-pumped distributed Raman amplifier (DRA) over 50 km of nonzero dispersion-shifted fiber with a zero dispersion wavelength of 1497 nm. The 100-mW pump Fabry–Pérot (FP) spectra centered at 1440, 1450, and 1460 nm are reproduced via FWM around the single-wavelength probe signal around 1558, 1548, and 1538 nm, respectively. The suppression of DRA gain by about 2–3 dB was experimentally observed with peak FWM at minimum phase mismatching between two 14xx-nm FP pump wavelengths and two 15xx-nm signal wavelengths. This DRA gain suppression, together with the reproduced pump FP spectrum at 15xx-nm signal band, may limit the usefulness of the forward-pumped DRA, generating spectrally nonuniform FWM-induced noise floors and crosstalk in wavelength-division-multiplexed fiber-optic transmission systems.**

***Index Terms*—Distributed Raman amplifier (DRA), four-wave mixing (FWM), nonzero dispersion-shifted fiber (NZ-DSF).**

I. Introduction

DISTRIBUTED RAMAN amplification (DRA) has the potential to extend the span length and the number of wavelength-division-multiplexed (WDM) channels for a high-capacity long-haul optical transmission system. It provides wide-band (∼100-nm) amplification of the optical signal in the transmission fiber using multiple high-power pumps of different wavelengths, about 100 nm shorter than that of the wide spectral width of the WDM carrier wavelengths. Back-pumped DRA has been widely used in transmission system experiments [1], [2], providing an equivalent lump amplifier noise figure $<$ 0 dB [3] and reducing the pump noises as averaged by the forward-traveling signal, whereas forward-pumped DRA allows the launched signal power to be reduced, which lessens the impact of optical nonlinearities on the transmission system [4]. Bidirectional-pumped DRA has the potential to provide more uniform Raman gain to overcome the fiber loss, which then reduces signal power for a given transmission span loss and mitigates fiber nonlinear effects [5].

A nondegenerated FWM of three pumps to generate a fourth signal wavelength for forward- and backward-pumped DRAs was experimentally observed over 50 km of true-wave (TW) fiber [6]. A degenerated FWM of two pump wavelengths to generate a third signal wavelength for the backward-pumped DRA was obtained over 80 km of TW fiber [7]. Severe degradation of the optical signal-to-noise ratio (OSNR) via elevated noise floors from FWM between pumps and signals [8] was experimentally observed in a bidirectionally pumped DRA over a 100-km nonzero dispersion-shifted fiber (NZ-DSF) with a zero-dispersion wavelength lying midway between copropagating pumps and signals.

In our work, we investigated nondegenerated FWM between two of the pump Fabry–Pérot (FP) wavelengths around 14xx nm and the single-wavelength probe signal around 15xx nm to generate unwanted FP spectra adjacent to the 15xx-nm probe signal. The pump FP spectra centered at 1440, 1450, and 1460 nm were experimentally reproduced via efficient FWM around the 1-mW single-wavelength probe signal at 1558, 1548, and 1538 nm, respectively. The suppression of DRA ON/OFF gain by about 2–3 dB was experimentally observed as FWM was maximized for reproduction of FP spectra at minimum phase mismatching between two FP pump wavelengths and two signal wavelengths. The Raman-enhanced pump-signal FWM was observed in [8] at various pump powers $>$155 mW, with more pump powers leading to more direct amplification of the FWM noise. In our forward-pumped DRA with three pumps each operating at a low pump power of 100 mW, more FWM were observed with a lower dispersion pump (1460 nm) and signal (1538 nm) wavelengths closer to the fiber zero-dispersion wavelength (1497 nm). The DRA gain suppression, together with the reproduced FP spectrum at 15xx-nm signal band, may limit the usefulness of the forward-pumped DRA, generating spectrally nonuniform FWM-induced noise floors and crosstalk in WDM fiber-optic transmission systems.

II. Phase Matching and FWM Efficiency

FWM is a third-order nonlinear parametric process, with second-order nonlinearity very small in an isotropic silica fiber. Significant FWM process occurs only if conservations of photon energy and photon momentum among the four guided optical waves are held. Consider the mixing of two pump photons $hf_{p'}$ and hf_p with a signal photon hf_s to generate a fourth optical photon $hf_{s'}$. To conserve the photon energy, this fourth photon has its optical frequency

$$f_{s'} = f_{p'} - f_p + fs. \tag{1}$$

This expression can be written as $\Delta f = f_{s'} - f_s = f_{p'} - f_p$, with the frequency difference in the pump being the same as that of the signal in this nondegenerated FWM.

Manuscript received July 9, 2002; revised February 21, 2003. This research was supported by the National Science Council, Taiwan, China under Contract NSC91-2215-E-009-054 and the Academic Excellence Program, Ministry of Education, Taiwan, China, under Contract 91-E-FA06-1-4-91X023.

T.-T. Kung is with the Institute of Electro-Optical Engineering, Hsinchu, Taiwan 30050, China.

C.-T. Chang is with San Diego State University, San Diego, CA 92182-4313 USA.

J.-C. Dung and S. Chi are with the National Chiao-Tung University, Taiwan, China.

Digital Object Identifier 10.1109/JLT.2003.810929

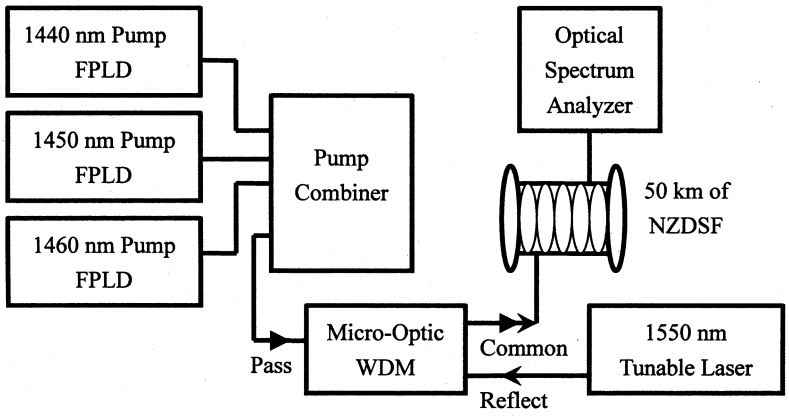

Fig. 1. Experimental setup for the forward pumped DRA.

Let β be the guided-wave propagation constant and $n(f_i)$ be the guided-wave phase index at the optical carrier frequency f_i; then the corresponding guided-wave photon momentum is $\hbar\beta_i = \hbar(2\pi f_i/c)n(f_i)$. The photon momentum conservation for the peak FWM is just $\Delta\beta = (\beta_{p'} - \beta_p) - (\beta_{s'} - \beta_s) = 0$. In a single-mode fiber (SMF), it is difficult to achieve both conservations of photon energy and momentum. The photon energy has to be conserved completely, since there is no uncertainty in frequency associated with an infinite long time for FWM in the nonlinear fiber-optic transmission experiments. With FWM occurring within the effective length of the fiber determined by attenuation and length of the fiber, the photon momentum is not completely conserved with a finite mismatching $\Delta\beta$. Expanding the propagation constants $\beta_{p'}$ and $\beta_{s'}$ in the Taylor series, respectively, around f_p and f_s and then retaining terms up to the third order in Δf, the propagation constant mismatch can be written as

$$\begin{aligned}\Delta\beta &= (\beta_{p'} - \beta_p) - (\beta_{s'} - \beta_s) \\ &= \Delta\beta_1 + \Delta\beta_2 + \Delta\beta_3 \end{aligned} \tag{2}$$

where

$$\Delta\beta_1 = \frac{2\pi}{c}\Delta f(N_p - N_s) \tag{3}$$

$$\Delta\beta_2 = \frac{\pi}{c}(\Delta f)^2\left(\lambda_s^2 D_s - \lambda_p^2 D_p\right) \tag{4}$$

and

$$\Delta\beta_3 = \frac{\pi}{3c^2}(\Delta f)^3\left[\left(2\lambda_p^3 D_p - 2\lambda_s^3 D_s\right) + \left(\lambda_p^4\frac{dD_p}{d\lambda_p} - \lambda_s^4\frac{dD_s}{d\lambda_s}\right)\right]. \tag{5}$$

The notations $\Delta\beta_1$, $\Delta\beta_2$, and $\Delta\beta_3$ are the first-, second-, and third-order terms, respectively, from the Taylor expansion of $\Delta\beta$ in terms of Δf. Here N_p and N_s are the group indexes for pump and signal, respectively. The fiber chromatic dispersion is $D = (1/c)(dN/d\lambda)$, and the dispersion slope is

$$\frac{dD}{d\lambda} = \frac{1}{c}\frac{d^2N}{d\lambda^2}.$$

Extending the analysis of FWM [9]–[12] to the case of two pump waves having identical attenuation α_p to mix with a single-wavelength signal wave with attenuation α_s, we obtain the FWM-generated optical power at frequency $f_{s'}$ through a fiber length of L km as

$$P_{s'}(L) = \frac{\eta}{9}d^2\gamma^2 P_p P_{p'} P_s \exp(-\alpha_s L)(L_{\text{eff}}^p)^2 \tag{6}$$

where the effective length for the pump is

$$L_{\text{eff}}^p = \frac{1 - \exp(-\alpha_p L)}{\alpha_p} \tag{7}$$

and the FWM efficiency is

$$\begin{aligned}\eta &= \frac{\alpha_p^2}{\alpha_p^2 + (\Delta\beta)^2}\left\{1 + \frac{4\exp(-\alpha_p L)\sin^2\left(\frac{\Delta\beta L}{2}\right)}{\left[1 - \exp(-\alpha_p L)\right]^2}\right\} \\ &\cong \frac{1}{1 + \left(\frac{\Delta\beta}{\alpha_p}\right)^2}. \end{aligned} \tag{8}$$

The notations P_p, $P_{p'}$, and P_s in (6) are the input powers at frequencies f_p, $f_{p'}$, and f_s, respectively. The approximation in (8) is valid under the condition of $\alpha_p L \gg 1$. The degeneracy factor d equals to 6 for a nondegenerated FWM analyzed here. The nonlinear coefficient γ [13] is

$$\gamma = \frac{2\pi n_2}{\lambda_s A_{\text{eff}}} \tag{9}$$

where A_{eff} is the effective mode field area, λ_s is the vacuum signal wavelength, and n_2 is the nonlinear-index coefficient.

III. Experiments and Discussion

A. Experimental Setup

Fig. 1 shows the experimental setup. The probe signal was from a mode-locked laser tunable from 1520 to 1600 nm with a relative intensity noise (RIN) of −145 dB/Hz. Three high-power (100-mW) pump laser diodes (LDs) have multiple FP wavelengths centered at 1440, 1450, and 1460 nm, respectively, each with its center wavelength stabilized by an external fiber Bragg grating (FBG). Fig. 2 shows the FP spectrum of the 1440-nm pump laser with a 0.225-nm mode spacing. These three pump lasers were combined in a pump combiner and then coupled to a reflection-type microoptic wavelength-division multiplexer for

forward pumping to a 50-km NZ-DSF having a mode-field area $A_{\text{eff}} = 73.7\ \mu\text{m}^2$ and a 1497-nm zero-dispersion wavelength, providing distributed Raman gain for the 15xx-nm signal.

B. Raman Gain

With a 15xx- nm tunable probe signal of 1-mW copropagating with the 100-mW pump, the ON/OFF distributed Raman gain spectra in Fig. 3 was obtained from the ratio of the measured fiber output powers with the pump being turned ON and OFF. There was a dip of about 2–3 dB in the ON/OFF Raman gain spectra associated with peak FWM at 1558, 1548, and 1538 nm for 1440-, 1450-, and 1460-nm pumps, respectively. The ON/OFF Raman gain peak for each pump wavelength is shifted from the pump wavelength by about 100 nm, having a peak gain of 3.6, 3.5, and 3.3 dB at a wavelength of 1540, 1550, and 1560 nm obtained from a 100-mW pumping individually at 1440, 1450, and 1460 nm, respectively.

The ON/OFF peak Raman amplification [14] is

$$G_A = \exp\left(\frac{g_R P_0 L_{\text{eff}}^p}{2A_{\text{eff}}}\right) \tag{10}$$

where g_R is the peak Raman gain coefficient, P_0 is the pump power at the amplifier input, and the pump effective length L_{eff}^p is given by (7). The factor 1/2 in the exponent of (10) is due to random polarization angle between pump and signal, spectrally separated by $\cong$ 100 nm, during their propagation in the 50-km fiber. With $g_R = 7.4 \times 10^{-14}$ m/W [15], [16] for the 1450-nm pump, $P_o = 100$ mW, $\alpha_p = 0.26$ dB/km, $L = 50$ km, $L_{\text{eff}}^p = 15.87$ km, and $A_{\text{eff}} = 73.7\ \mu\text{m}^2$, the peak amplification from (10) is $G_A = 2.22$ or 3.46 dB, which is very close to the measured gain of 3.5 dB in Fig. 3.

C. FWM in a DRA

For a 100-mW pump at 1440-nm forward traveling through the 50-km NZDSF with the 1-mW single-wavelength probe signal, the three output signal spectra in Fig. 4(a) show the additional side lobes at the probe single-wavelength signal centered at 1554, 1558, and 1562 nm due to FWM of the pumps and signal. Fig. 4(b) is the same as Fig. 4(a), except it is for the 1450-nm pump of 100 mW copropagating with probe signal centered at 1544, 1548, and 1552 nm, while Fig. 4(c) is for the 1460-nm pump of 100 mW and the probe signal centered at 1534, 1538, and 1542 nm. It is interesting that the FP signal spectra associated with the most efficient FWM and the corresponding FP pump spectra were spectrally separated by 118, 98, and 78 nm, respectively, in Fig. 4(a)–(c), solely determined by the fiber group delay and dispersion characteristics to be discussed subsequently.

The reproduction of the FP spectra in the 15xx-nm signal band via FWM was not observed for the single-mode fiber (SMF-28), DSF, and dispersion-compensated fiber (DCF) with zero-dispersion wavelengths at 1310, 1547, and 1710 nm, respectively. This is in drastic contrast with the forward-pumped DRA with the NZ-DSF having a zero-dispersion wavelength of 1497 nm, reproducing FP pump spectra in the 15xx-nm signal band via FWM.

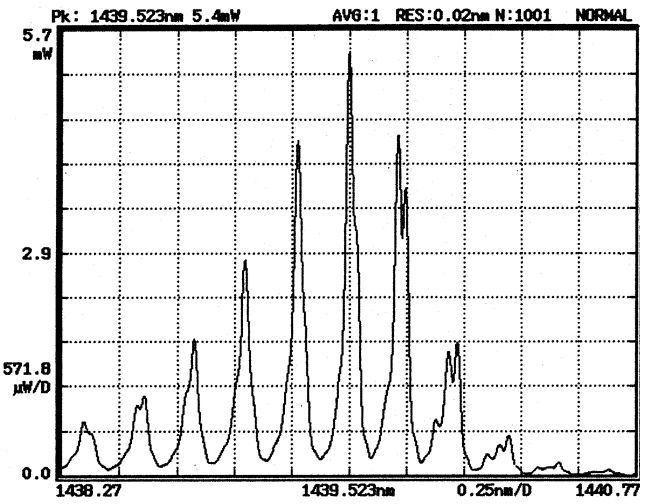

Fig. 2. The FP mode spectrum (mode spacing = 0.225 nm) of the 1440-nm pump laser.

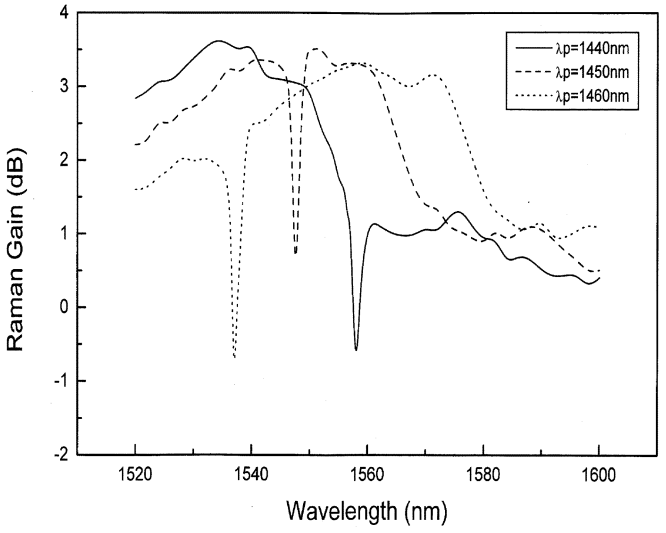

Fig. 3. The ON/OFF distributed Raman gain spectra for 1440-, 1450-, and 1460-nm pump wavelengths with each of the 100-mW pump power copropagated with a 1 mW of 15xx-nm signal. The Raman gain was obtained from the ratio of the measured fiber output powers with the pump being turned ON and OFF.

D. Delay and Dispersion in the NZ-DSF

To further support our understanding of the phase mismatching in FWM, the chromatic dispersion and the group delay (solid lines) versus wavelength in Fig. 5 were measured by the optical network analyzer from 1525 to 1635 nm for a 300-m-long NZ-DSF. The zero-dispersion wavelength of 1497 nm is just the wavelength for minimum group delay. The group delays (solid square) at 14xx nm in Fig. 5 were inferred from that of the corresponding signal wavelengths at 15xx nm obtained from maximization of FWM efficiency for reproduction of FP spectra to be discussed subsequently, showing the group delays at pump wavelengths of 1440, 1450, and 1460 nm to be the same as that of the signal wavelengths of 1558, 1548, and 1538 nm, respectively. Since the measured dispersion versus wavelength seems linear, we made a linear

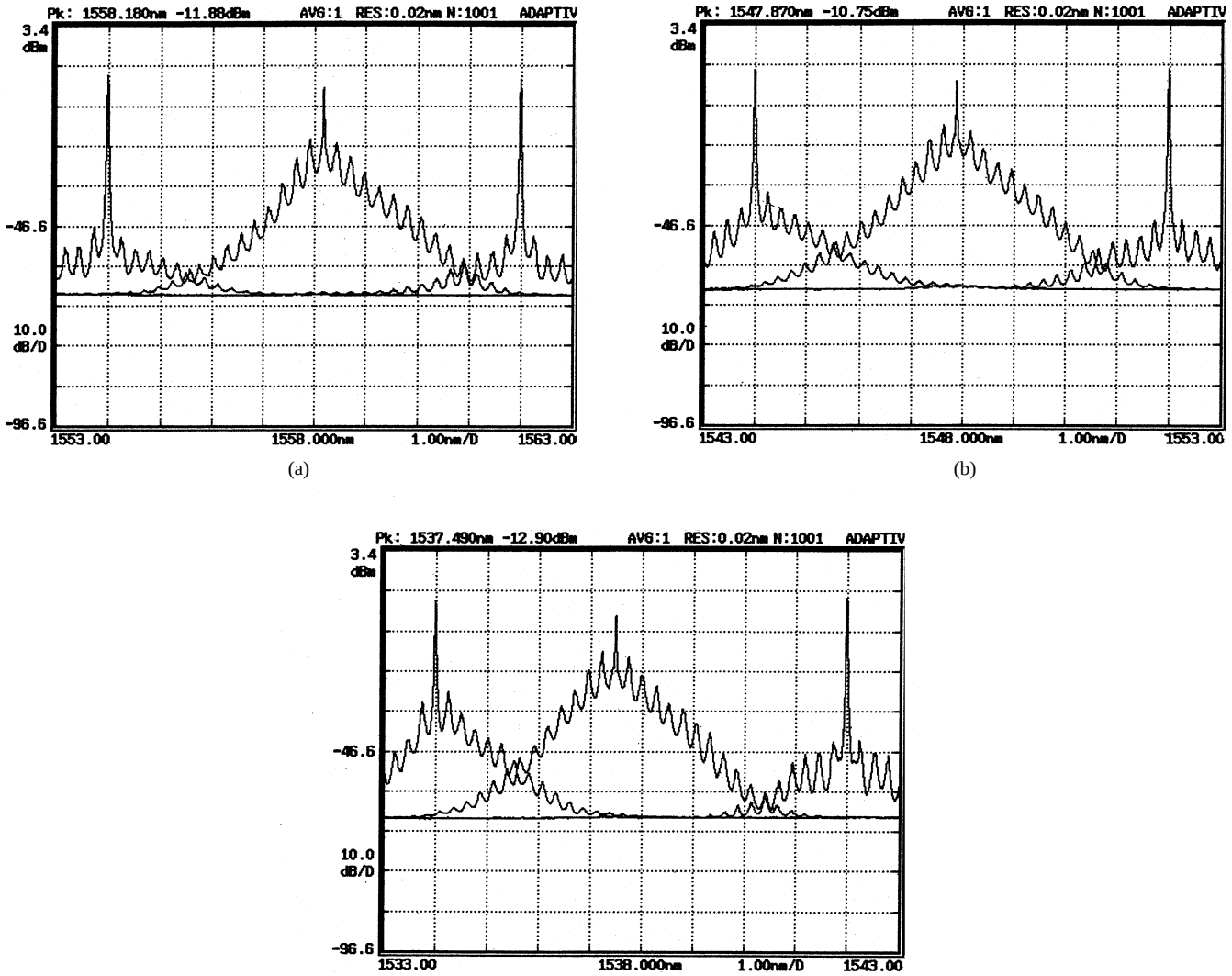

Fig. 4. FWM reproduced spectra for a 100-mW pump-power forward traveling with 1-mW single-wavelength probe signal through a 50-km NZ-DSF with a zero-dispersion wavelength of 1497 nm: (a) 1440-nm pump with the probe single-wavelength signal centered at 1554, 1558, and 1562 nm; (b) 1450-nm pump with probe signal centered at 1544, 1548, and 1552 nm; and (c) 1460-nm pump with the probe signal centered at 1534, 1538, and 1542 nm.

extrapolation to the shorter wavelength down to 1440 nm and obtained a zero-dispersion wavelength of 1497 nm consistent with the manufacturer specification of 1497.3 nm.

E. Photon Energy and Momentum Conservations in FWM

The pump FP mode centered at 1440 nm is reproduced via FWM at the signal band centered at 1558 nm, resulting in identical pump and signal FP mode spacing with $\Delta f = 32.6$ GHz as shown in Figs. 2 and 4(a). Thus, the photon energy conservation is completely satisfied in the FWM experiment here, having $f_{p'} = f_p + 32.6$ GHz and $f_{s'} = f_s + 32.6$ GHz, as illustrated in the inset of Fig. 5. The momentum conservation with $\Delta\beta \to 0$ is also required for efficient FWM with high η [see (8)].

The fiber group delay versus wavelength (from 1440 to 1580 nm) in Fig. 5 is U-shaped with minimum delay at the wavelength of 1497 nm or the zero-dispersion wavelength. For a maximum mixing efficiency η, the phase mismatch $\Delta\beta$ has to be minimized with the first-order mismatch $\Delta\beta = (2\pi/c)(\Delta f(N_p(f_p) - N_s(f_s))) = 0$ [see (3)]. This then implies that the group delays at $\lambda_p = 1440$, 1450, and 1460 nm are identical to that at $\lambda_s = 1558$, 1548, and 1538 nm, respectively, as shown in Fig. 5. Thus, the second-order term in (4) dominates the phase mismatch with $\Delta\beta_{\min} = \Delta\beta_2 =$ 0.25, 0.21, and 0.16 km^{-1} at 1558, 1548, and 1538 nm, respectively, as shown in Table I. The residual mismatch $\Delta\beta_{\min} \neq 0$ for maximizing reproduction of FP spectra via FWM, since $N_p(f_p + 32.6\,\text{GHz}) > N_s(f_s + 32.6\,\text{GHz})$ or $N_p(f_p - 32.6\,\text{GHz}) < N_s(f_s - 32.6\,\text{GHz})$ in the U-shaped group delay versus wavelength curve, as shown in the inset of Fig. 5. The third-order term $\Delta\beta_3$ from (5) was estimated to be negligibly small (about $-8.0 \times 10^{-5}\text{km}^{-1}$).

Since we do not have the measured group indexes at the 14xx-nm pump wavelength, we evaluate nonminimum $\Delta\beta$

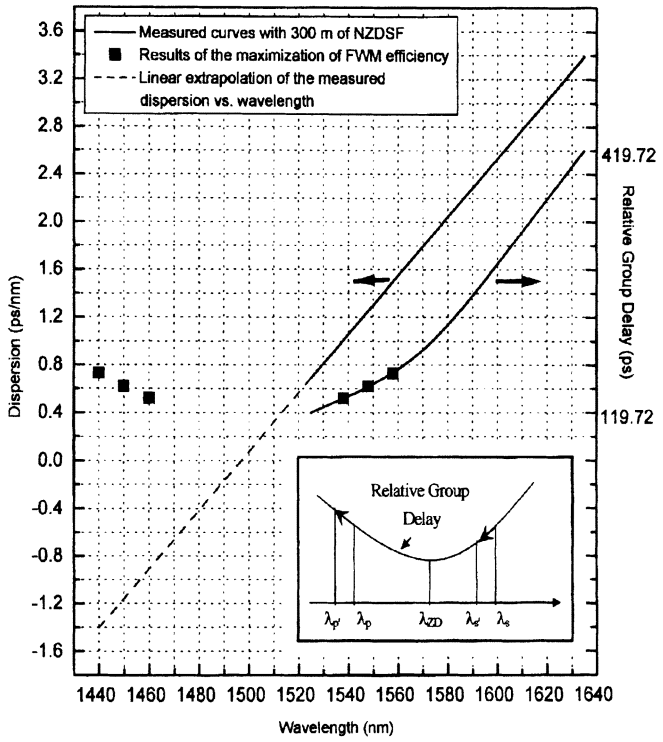

Fig. 5. The dispersion and relative group delay of a 300-m NZ-DSF. The solid line measured by an optical network analyzer and the solid squares are the results inferred from the maximum FWM efficiency for reproduction of FP spectra. The dashed line is a linearly extrapolated dispersion versus wavelength.

from the dispersion at the signal band, as described subsequently. With the group index N_p at 14xx-nm pump being identical to the 15xx-nm signal group index N_{s0} for maximum FWM, $\Delta\beta$ in (3) can be written as

$$\Delta\beta = \frac{2\pi}{c}\Delta f(N_{s0} - N_s) = 2\pi\Delta f \cdot D_s \cdot \Delta\lambda_{s_0,s} \qquad (11)$$

where $\Delta\lambda_{s_0,s} = \lambda_{s0} - \lambda_s$, and D_s is the dispersion evaluated at $(\lambda_{s0} + \lambda_s)/2$.

Table I also shows $\Delta\beta$ obtained from (11) with $\Delta f = 32.6$ GHz, $\Delta\lambda_{s_0,s} = 4$ nm, and D_s from Fig. 5. A positive (negative) $\Delta\beta$ indicates that the 14xx-nm pump group index is higher (lower) than the 15xx-nm signal group index at a shorter (longer) signal wavelength.

As the 1-mW probe signal wavelength was varied, more FP wavelengths were regenerated and a dip in the ON/OFF DRA gain of about 2 dB was observed at the signal wavelength of 1558 nm in Fig. 4(a). It is due to the reduction of the probe signal by peak FWM for reproduction of FP spectra with $\eta = 5.4\%$ from (8) for a minimum phase mismatch $\Delta\beta = \Delta\beta_2 = 0.25\ \text{km}^{-1}$. Raman gains in Fig. 3 are reduced to -0.5, 0.8, and -0.8 dB by the dips of 2.0, 2.6, and 3.0 dB at 1558, 1548 and 1538 nm, respectively. The increase of dip is due to less residual phase mismatch $\Delta\beta_2$ of 0.25, 0.21, and 0.16 km^{-1}, with decreasing signal wavelength, as shown in Table I. Thus, we conclude that more reduction of Raman gain is associated with more FWM due to less dispersion at the wavelength closer to the zero-dispersion wavelength. The reduced Raman gain is $+0.8$ dB at 1548 nm, very close to the Raman gain peak of the 1450-nm pump, while the two other reduced gains are both negative, -0.5 dB at 1558 nm and -0.8 dB at 1538 nm, since they are about 20 nm away from the corresponding gain peak wavelengths associated with 1440- and 1460-nm pumps.

Table I also shows that less FWM efficiency $\eta = 2.2 \times 10^{-4}$ and 1.9×10^{-4} [from (8)] are associated with more phase mismatch $\Delta\beta = 4.1\ \text{km}^{-1}$ and $-4.3\ \text{km}^{-1}$ [from (4)], respectively, for the probe single-wavelength signals at 1554 and 1562 nm. Thus, there were fewer FP wavelengths generated and a negligible dip in the DRA gain in Fig. 4(a).

For the pumps at 1450 and 1460 nm, the maximum FWM for the reproduction of FP spectra was experimentally observed as in Fig. 4(b) and (c) at 1548 and 1538 nm, respectively. This, in turn, implies that the group indexes at 1450 and 1460 nm are identical to that at 1548 and 1538 nm, respectively, solely determined by the NZ-DSF group-delay characteristics.

F. FWM-Generated Power

Among the three FP spectra having a maximum number of reproduced FP wavelengths at the center of Fig. 4, the FWM efficiency is highest at 1538 nm due to the lowest $\Delta\beta = \Delta\beta_2 = 0.16\ \text{km}^{-1}$ (see Table I) associated with the lowest dispersion, since both pump of 1460 nm and signal wavelengths of 1538 nm are most close to the zero-dispersion wavelength of 1497 nm in our experiments.

Comparing two side FP spectra in each of the three graphs in Fig. 4, more FWM at a shorter wavelength is due to lower $\Delta\beta$ associated with lower dispersion, resulting in a higher η, as shown in Table I.

Comparing six side spectra in Fig. 4, the longest probe wavelength at 1562 nm has the lowest FWM efficiency due to the highest $\Delta\beta = -4.3\ \text{km}^{-1}$ associated with the highest dispersion at 1562 nm, while the highest FWM efficiency at 1534 nm is associated with the lowest $\Delta\beta = 2.7\ \text{km}^{-1}$ or the lowest dispersion, as shown in Table I.

We assume the same Raman gain G for the probe signal and the FWM-generated signal, since FWM occurs at the fiber length $z \ll L_{\text{eff}}/2$ with FWM proportional to $P_{p'}P_p$. The FWM-generated power $P_{s'}(L)$ normalized to the transmitted signal power $P_s(L) = P_s(0)\exp(-\alpha_s L)$ can be obtained from (6) –(8). The nine constituent FP pump powers in Fig. 2 were 2.37, 7.04, 17.51, 21.49, 17.11, 10.75, 6.77, 4.42, and 3.08 mW, from long to short wavelengths. Each pump power is estimated from the optical spectrum analyzer (OSA) measured power, with 0.02-nm resolution, integrated over the spectral width of 0.2 nm for each FP wavelength. The nonlinear coefficient $\gamma = (2\pi n_2)/(\lambda_s A_{\text{eff}}) = 1.5\ \text{W}^{-1}\text{km}^{-1}$ is obtained using $n_2 = 2.7 \times 10^{-20}\ \text{m}^2\text{W}^{-1}$ [17] and $A_{\text{eff}} = 73.7\mu\text{m}^2$. The fiber attenuations are $\alpha_p = 0.26$ dB/km and $\alpha_s = 0.19$ dB/km. The FWM efficiencies for 1554, 1558, and 1562 nm are estimated from (8) to be 2.18×10^{-4}, 0.0545, and 1.94×10^{-4}, respectively. Assuming a random polarization angle between pump and signal copropagating over the 50-km fiber, we multiply a factor 1/2 to (6) and then include the product counts for two adjacent FP wavelengths (with frequency spacing Δf) to obtain the normalized FWM-generated output power at $f_s + \Delta f$ as

$$\frac{P_{s+1}(L)}{P_s(L)} = \frac{1}{2} \cdot \frac{\eta}{9} d^2\gamma^2 (L_{\text{eff}})^2 (P_p P_{p-1} + P_p P_{p+1}). \qquad (12)$$

TABLE I
ESTIMATED VALUES OF THE PHASE MISMATCH $\Delta\beta$ AND THE FWM EFFICIENCY η FOR ($\lambda_p = 1440$ nm, $\lambda_s = 1554$, 1558, AND 1562 nm), ($\lambda_p = 1450$ nm, $\lambda_s = 1544$, 1548, AND 1552 nm), AND ($\lambda_p = 1460$ nm, $\lambda_s = 1534$, 1538, AND 1542 nm)

λ_p (nm)	D_p (ps/nm-km)	λ_s (nm)	D_s (ps/nm-km)	$\Delta\beta_1$ (km^{-1})	$\Delta\beta_2$ (km^{-1})	$\Delta\beta_3$ (km^{-1})	$\Delta\beta$ (km^{-1})	η
		1562	5.3				-4.31	1.94×10^{-4}
1440	-4.7	1558	5.0	0	0.25	-8.2×10^{-5}	0.25	0.0545
		1554	4.7				4.06	2.18×10^{-4}
		1552	4.5				-3.65	2.70×10^{-4}
1450	-3.9	1548	4.2	0	0.21	-6.8×10^{-5}	0.21	0.0755
		1544	3.8				3.32	3.27×10^{-4}
		1542	3.7				-2.99	4.03×10^{-4}
1460	-3.0	1538	3.4	0	0.16	-5.4×10^{-5}	0.16	0.1233
		1534	3.0				2.65	5.12×10^{-4}

(D_s at 1536, 1540, 1546, 1550, 1556, 1560 nm are 3.2, 3.6, 4.0, 4.4, 4.9, 5.2 ps/nm-km, respectively)

We neglect the contributions to (12) from $2\Delta f$ and higher FP frequency spacing, since their contributions to the FWM efficiency in (8) are at least $\ll 1/4$ lower than that of Δf. Based upon numerical values in Table I for the adjacent FP spacing $\Delta f = 32.6$ GHz, we find from (12) the largest normalized FWM-generated power normalized to the probe signal power at 1554, 1558, and 1562 nm to be -37.51, -13.51, and -38.01 dB, respectively. The corresponding measured powers for the highest FWM-generated FP wavelengths from Fig. 5(a) were -36.92, -12.31, and -37.69 dB, as compared with the probe 1-mW signals.

IV. CONCLUSION

Peak FWM for reproduction of the FP spectra was observed for mixing the FP modes of 1440-, 1450-, and 1460-nm pumps, respectively, with 1558-, 1548-, and 1538-nm single-wavelength signals in a forward-pumped DRA over a 50-km NZ-DSF with a zero-dispersion wavelength at 1497 nm or the minimum of the U-shaped fiber group delay versus wavelength curve. This is the consequence of a minimum phase mismatch for FWM due to equal group delay for the pump (1440 nm, for example) and its corresponding probe signal wavelength (1558 nm, correspondingly), solely determined by the fiber group delay or dispersion characteristics. The pump wavelength (1460 nm, for example) closer to 1497 nm with smaller fiber dispersion and less phase mismatch will have the largest FWM efficiency around the signal wavelength (1538 nm, correspondingly). More FP spectra were regenerated together with the suppression of an ON/OFF DRA gain of about 2–3 dB was observed at the peak FWM signal wavelength. This DRA gain suppression, together with the reproduced pump FP spectrum at 15xx-nm signal band, may limit the usefulness of the forward-pumped DRA, generating spectrally nonuniform FWM-induced noise floors and crosstalk in WDM fiber-optic transmission systems.

REFERENCES

[1] I. Haxell, N. Robinson, A. Akhtar, M. Ding, and R. Haigh, "2410 km all-optical network field trial with 10 Gb/s DWDM transmission," in *Proc. OFC'2000*, Baltimore, MD, 2000, PD41-1.

[2] F. Koch, S. V. Chernikov, S. A. E. Lewis, and J. R. Taylor, "Characterization of single stage, dual-pumped Raman fiber amplifiers for different gain fiber lengths," *Electron. Lett.*, vol. 36, no. 4, pp. 347–348, 2000.

[3] P. B. Hansen, L. Eskildsen, A. J. Stentz, T. A. Strasser, J. Judkins, J. J. Demarco, R. Pedrazzani, and D. J. DiGiovanni, "Rayleigh scattering limitations in distributed Raman pre-amplifier," *IEEE Photon. Technol. Lett.*, vol. 10, pp. 159–161, Jan. 1998.

[4] R. P. Espindola, K. L. Bacher, K. Kojima, N. Chand, S. Srinivasan, G. C. Cho, F. Jin, C. Fuchs, V. Milner, and W. C. Dautremont-Smith, "Penalty-free 10 Gbits/s single-channel co-pumped distributed Raman amplification using low RIN 14xx nm DFB pump," *Electron. Lett.*, vol. 38, no. 3, pp. 113–115, 2002.

[5] N. Takachio and H. Suzuki, "Application of Raman-distributed amplification to WDM transmission systems using 1.55-μm dispersion-shifted fiber," *J. Lightwave Technol.*, vol. 19, pp. 60–69, Jan. 2001.

[6] R. E. Neuhauser, P. M. Krummrich, H. Bock, and C. Glingener, "Impact of nonlinear pump interactions on broadband distributed Raman amplification," in *Proc. OFC'2001*, Anaheim, CA, 2001, MA4-1.

[7] C. R. S. Fludger, V. Handerek, N. Jolley, and R. J. Mears, "Novel ultra-broadband high performance distributed Raman amplifier employing pump modulation," in *Proc. OFC'2002*, Anaheim, CA, 2002, WB4, pp. 183–184.

[8] J. Bromage, P. J. Winzer, L. E. Nelson, and C. J. McKinstrie, "Raman-enhanced pump-signal four-wave mixing in bidirectionally-pumped Raman amplifiers," in *OAA'2002*, Vancouver, Canada, 2002, OWA5-1.

[9] K. O. Hill, D. C. Johnson, B. S. Kawasaki, and R. I. MacDonald, "CW three-wave mixing in single-mode optical fibers," *J. Appl. Phys.*, vol. 49, no. 10, pp. 5098–5106, 1978.

[10] N. Shibata, R. P. Braun, and R. G. Waarts, "Phase-mismatch dependence of efficiency of wave generation through four-wave mixing in a single-mode optical fiber," *J. Quantum Electron.*, vol. 23, no. 7, pp. 1205–1210, 1987.

[11] R. W. Tkach, A. R. Chraplyvy, F. Forghieri, A. H. Gnauck, and R. M. Derosier, "Four-photon mixing and high-speed WDM systems," *J. Lightwave Technol.*, vol. 13, pp. 841–849, May 1995.

[12] S. Song, C. T. Allen, K. R. Demarest, and R. Hui, "Intensity-dependent phase-matching effects on four-wave mixing in optical fibers," *J. Lightwave Technol.*, vol. 17, pp. 2285–2290, Nov. 1999.
[13] G. P. Agrawal, *Nonlinear Fiber Optics*. San Diego, CA: Academic, 1995, p. 42.
[14] ——, *Nonlinear Fiber Optics*. San Diego, CA: Academic, 1995, p. 330.
[15] J. Bromage, K. Rottwitt, and M. E. Lines, "A method to predict the Raman gain spectra of germanosilicate fibers with arbitrary index profiles," *IEEE Photon. Technol. Lett.*, vol. 14, pp. 24–26, Jan. 2002.
[16] H. Kidorf, K. Rottwitt, M. Nissov, M. Ma, and E. Rabarijaona, "Pump interactions in a 100-nm bandwidth Raman amplifier," *IEEE Photon. Technol. Lett.*, vol. 11, pp. 530–532, May 1999.
[17] J. C. Antona, S. Bigo, and S. Kosmalski, "Nonlinear index measurements of various fiber types over C + L bands using four-wave mixing," in *Proc. ECOC'01*, Amsterdam, The Netherlands, 2001, pp. 270–271.

Tsu-Te Kung was born in Taoyuan, Taiwan, in 1962. He received the B.S. degree in physics from Tamkang University, Taiwan, China, in 1985 and the M.S. degree in optoelectronics from National Chiao-Tung University, Taiwan, China, in 1987. He is currently working toward the Ph.D. degree with the Institute of Electro-Optical Engineering, National Chiao-Tung University.

From 1989 to 1991, he was an Assistant Researcher at the Telecommunications Laboratories, Chung-Li, Taiwan, China, where he engaged in research in the area of erbium-doped fiber amplifiers. Since 1992, he has been with the faculty of the National Lien-Ho Institute of Technology, Miaoli, Taiwan. Currently, he is a Lecturer of electrooptical engineering, National Lien-Ho Institute of Technology. He is interested in nonlinear fiber optics.

Ching-Ten Chang (S'73–M'75) received the Ph.D. degree in electrical engineering from the University of Washington, Seattle, in 1975.

As a Research Associate with the University of Washington from 1975 to 1977, he conducted research in optical holography and fiber optics. He joined the Naval Ocean Systems Center, San Diego, CA, in 1979. He is curently a Professor of electrical and computer engineering at San Diego State University, San Diego, CA. His research interests have been in optical fiber communications, fiber-optic delay lines, and heterostructure lasers.

Jeng-Cherng Dung was born in Pingtung, Taiwan, China, in 1963. He received the B.S. degree in physics from the National Tsing-Hua University, Taiwan, China, in 1986 and the Ph.D. degree in optoelectronics from the National Chiao-Tung University, Taiwan, China, in 1996.

He is currently an Assistant Professor in National Chiao-Tung University, where he works on the fiber circulating loop testbed, soliton transmission, and broad-band Raman amplifiers. His research interests are optical amplifier and optical fiber communications.

Sien Chi received the B.S.E.E. degree from National Taiwan University, Taiwan, China, in 1959, the M.S.E.E. degree from National Chiao-Tung University, Taiwan, China, in 1961, and the Ph.D. degree in electrophysics from the Polytechnic Institute of Brooklyn, NY, in 1971.

He joined the Faculty of National Chiao-Tung University, and he was Chair of the Department of Electrophysics from 1972 to 1973. From 1973 to 1977, he was Director of the Institute of Electronics. From 1977 to 1978, he was a Resident Visitor at Bell Laboratories, Holmdel, NJ. From 1985 to 1988, he was the Principal Advisor with the Hua-Eng Company, and from 1988 to 1990, he was Director of the Institute of Electro-Optical Engineering. Currently, he is a Professor of electrooptical engineering, National Chiao-Tung University. His research interests are optical fiber communications, optical solitons, and optical fiber amplifiers.

Dr. Chi is a Fellow of the Optical Society of America (OSA) and the PSCA. He was the Symposium Chair of the International Symposium of Optoelectronics in Computer, Communications, and Control in 1992, which was co-organized by National Chiao-Tung University and the International Society for Optical Engineers (SPIE). From 1993 to 1996, he received the Distinguished Research award sponsored by the National Science Council, Taiwan. Since 1996, he has been the Chair Professor of the Foundation for the Advancement of Outstanding Scholarship.